Cy5.5-labeled Affibody molecule for near-infrared fluorescent optical imaging of epidermal growth factor receptor positive tumors

Zheng Miao
Gang Ren
Hongguang Liu
Lei Jiang
Zhen Cheng
Stanford University
Stanford Cancer Center
Molecular Imaging Program at Stanford
Department of Radiology and Bio-X Program
1201 Welch Road, Lucas Expansion, P095
Stanford, California 94305-5344

Abstract. Affibody protein is an engineered protein scaffold with a three-helical bundle structure. Affibody molecules of small size (7 kD) have great potential for targeting overexpressed cancer biomarkers *in vivo*. To develop an Affibody-based molecular probe for *in vivo* optical imaging of epidermal growth factor receptor (EGFR) positive tumors, an anti-EGFR Affibody molecule, Ac-Cys-$Z_{EGFR:1907}$ (7 kD), is site-specifically conjugated with a near-IR fluorescence dye, Cy5.5-mono-maleimide. Using fluorescent microscopy, the binding specificity of the probe Cy5.5-$Z_{EGFR:1907}$ is checked by a high-EGFR-expressing A431 cell and low-EGFR-expressing MCF7 cells. The binding affinity of Cy5.5-$Z_{EGFR:1907}$ (K_D) to EGFR is 43.6±8.4 nM, as determined by flow cytometry. For an *in vivo* imaging study, the probe shows fast tumor targeting and good tumor contrast as early as 0.5 h postinjection (p.i.) for A431 tumors, while MCF7 tumors are barely visible. An *ex vivo* imaging study also demonstrates that Cy5.5-$Z_{EGFR:1907}$ has high tumor, liver, and kidney uptakes at 24 h p.i.. In conclusion, Cy5.5-$Z_{EGFR:1907}$ shows good affinity and high specificity to the EGFR. There is rapid achievement of good tumor-to-normal-tissue contrasts of Cy5.5-$Z_{EGFR:1907}$, thus demonstrating its potential for EGFR-targeted molecular imaging of cancers.
 [DOI: 10.1117/1.3432738]

Keywords: optical materials; infrared imaging; fluorescence; targets; tissue; optics.

Paper 09476RR received Oct. 22, 2009; revised manuscript received Mar. 15, 2010; accepted for publication Mar. 23, 2010; published online Jun. 23, 2010.

1 Introduction

Epidermal growth factor receptor (EGFR) is a transmembrane protein belonging to ErbB oncogene family. Overexpression of EGFR has been frequently detected in a wide range of human tumors, for example, non-small-cell lung cancer, small-cell carcinoma of the head and neck, esophageal cancer, gastric cancer, gliomas, colon cancer, pancreas cancer, breast cancer, ovarian cancer, bladder cancer, kidney cancer, and prostate cancer.[1] Recently, EGFR has emerged as an attractive target for cancer therapy. EGFR-targeted therapies including the use of monoclonal antibodies (MAbs: cetuximab, panitumumab) and tyrosine kinase inhibitors [TKIs: gefitinib (Iressa), erlotinib (Tarceva), lapatinib (Tykerb)] have been developed and extensively studied.[2–4] Meanwhile, molecular probes for EGFR imaging have also been under active investigation.[5–7] It is expected that EGFR-specific molecular probes could potentially be used for early detection of EGFR positive tumors and metastases, prediction of efficacy for EGFR-targeted therapy, and for guidance in surgery etc.

A variety of small-molecule-based EGFR ligands and anti-EGFR antibodies are available for developing molecular probes for different imaging modalities. However, it has been found that small molecules labeled with radionuclides generally showed rapid blood clearance, but very low tumor uptake and poor tumor imaging quality.[5–7] Moreover, these small molecules are relatively sensitive to chemical modifications with large bulky tags, and they may not be a good platform for developing optical imaging probes for EGFR. On the other hand, fluorescent dyes or radiolabeled anti-EGFR MAbs have been prepared and have demonstrated good tumor uptake. However, because of slow tumor targeting ability and slow clearance[8–10] of the MAbs, the tumors can be visualized only at many hours or even days after injection of the probes. Substantial improvement of EGFR molecular probes is still required for preclinical and clinical applications.

Small protein scaffolds have shown great potential for recognizing a variety of biomarkers.[11,12] Among them Affibody molecules are a promising generalizable platform for developing imaging or therapeutic agents for different molecular targets.[13–15] Affibody molecules are small, engineered proteins with only 58 amino acid residues and a three-helix bundle scaffold structure, while they display a binding surface as large as antibodies. High-affinity Affibody proteins (lower nanomolar or even picomolar) against different targets could be obtained through the phage display technique and affinity

Address all correspondence to: Zhen Cheng, PhD, Molecular Imaging Program at Stanford, Department of Radiology and Bio-X Program, 1201 Welch Road, Lucas Expansion, P095 Stanford, California 94305. Tel: 650-723-7866; Fax: 650-736-7925; E-mail: zcheng@stanford.edu

1083-3668/2010/15(3)/036007/7/$25.00 © 2010 SPIE

maturation. Because of the small size (7 kDa) and high affinities, Affibody proteins generally show fast tumor targeting (within a half hour), high tumor uptake, and quick clearance from normal tissues. Moreover, Affibody proteins can be chemically synthesized with reasonable yield using conventional solid-phase peptide synthesis. Synthetic Affibodies retain the high binding specificity and affinity. Anti-human epidermal growth factor receptor 2 (HER2) Affibody molecules have been labeled with various radionuclides, organic dyes, and nanoparticles for imaging applications from cell to small animal imaging and even human.[16–18] Dual-dye-labeled Affibody or even tri-labeled Affibody have also been reported.[19] Overall, an Affibody protein scaffold has been proven to be an excellent platform for molecular probe development.

An anti-EGFR Affibody protein, $Z_{EGFR:1907}$, has shown strong binding (K_D=5.4 nM) to EGFR with no cross-binding to other growth factor receptors.[20] It has been found that ^{64}Cu- and ^{111}In-labeled $Z_{EGFR:1907}$ display fast and high tumor uptake (~10% inject dose (ID)/g and 3 to 6%ID/g, respectively, at 4 h p.i.), as well as quick clearance from blood pool (~5%ID/g and 1.5 to 2%ID/g, respectively, 4 h p.i.) and EGFR nonexpression tissues[20–24] (except kidney). We thus hypothesized that this Affibody could be a good protein for developing optical imaging probes for near-infrared (NIR) fluorescent imaging of EGFR positive tumors. In this research, a cysteine residue was first added to the N-terminus of $Z_{EGFR:1907}$. The resulting chemically synthesized protein, Ac-Cys-$Z_{EGFR:1907}$ (Ac-CVDNKFNKEMWAAWEEIRNLPNLNGWQMTAFIASLVDDPSQSANLLAEAKKLNDAQAPK-NH_2), was site specifically conjugated with a NIR dye, Cy5.5-mono-maleimide. The optical probe Cy5.5-$Z_{EGFR:1907}$ was further evaluated in the EGFR positive human epithelial carcinoma A431 cell culture and tumor-bearing mice.

2 Materials and Methods

2.1 *General Material and Reagent*

Cy5.5-mono-maleimide was purchased from GE Healthcare (Piscataway, New Jersey). Dichloromethane, triethylamine, N-hydroxybenzotriazole hydrate (HOBT), diisopropylcarbodiimide (DIC), ethyl acetate, and dithiothriotol (DTT) were purchased from Sigma-Aldrich Chemical Co. (St. Louis, Missouri). Dimethylsulfoxide (DMSO) and ethyl acetate were purchased from Fisher Scientific (Pittsburgh, Pennsylvania). All the other standard reagents were purchased from Sigma-Aldrich Chemical Co. All chemicals were used without further purification.

The Affibody analog, Ac-Cys-$Z_{EGFR:1907}$, was prepared by a solid phase peptide synthesis method as previously described.[21] Reverse-phase high-performance liquid chromatography (RP-HPLC) was performed on a Dionex Ultimate 3000 HPLC system (Dionex Corporation, Sunnyvale, California, for analysis and preparation of peptides and bioconjugates) equipped with a photodiode array detector. Five UV wavelengths (218, 254, 280, 500, and 675 nm) were monitored for all the experiments. Analytical RP-HPLC column from Sorbent Tech (Atlanta, Georgia) (Grace Vydac C4, 4.6 $\times$250 mm) was used for analysis of the labeled small protein. The mobile phase was solvent A, 0.1% trifluoroacetic acid (TFA)/H_2O, and solvent B, 0.1%TFA/acetonitrile. The flow rate was 1 mL/min, with the mobile phase starting from 80% solvent A and 20% solvent B (0 to 2 min) to 50% solvent A and 50% solvent B at 32 min. Matrix-assisted laser desorption/ionization time of flight mass spectrometry (MALDI-TOF-MS, model: Perseptive Voyager-DE RP Biospectrometer) (Framingham, Massachusetts) or an electrospray ionization quadrupole mass spectrometer (ESI-MS, model: Micromass ZQ single quadrupole LC-MS) (Milford, Massachusetts) was performed by the Stanford Protein and Nucleic Acid Biotechnology Facility and Stanford Chemistry Department Mass Spectrometry Facility, respectively. The human epithelial carcinoma cancer cell line A431 was obtained from the American Type Tissue Culture Collection (Manassas, Virginia). Female athymic nude mice (nu/nu) were purchased from Charles River Laboratories (Boston, Massachusetts).

2.2 *Synthesis of Cy5.5-$Z_{EGFR:1907}$*

The general procedure for preparation of Cy5.5-$Z_{EGFR:1907}$ is as follows. The Affibody molecule Ac-Cys-$Z_{EGFR:1907}$ was dissolved in freshly degassed phosphate buffer (0.1 M, pH 7.4) at a concentration of approximately 1 mg/mL. The NIR dye Cy5.5-mono-maleimide (300 μg) in DMSO was then added (1.5 equivalents per equivalent of the Affibody). After vortexing for 2 h, the reaction mixture was purified by the HPLC equipped with a Grace Vydac 214TP54-C4 column. Characterization of Cy5.5-$Z_{EGFR:1907}$ was confirmed using MALDI-TOF-MS. The purity of the bioconjugate was confirmed by the analytical HPLC.

Fluorescence emission of Cy5.5-$Z_{EGFR:1907}$ was measured on the Fluomax-3 fluorophotometer (HORIBA Jobin Yvon, Edison, New Jersey), and the spectrum was scanned from 650 to 850 nm with an increment of 1 nm. The wavelength of excitation light is 635 nm. The absorption spectrum of Cy5.5-$Z_{EGFR:1907}$ was recorded on an Agilent 8453 UV-visible ChemStation (Agilent Technologies, Wilmington, Delaware). The spectrum was scanned from 500 to 850 nm with an increment of 1 nm.

2.3 *Fluorescence Microscopy Study*

The A431 and MCF7 cells were cultured in high-glucose Dulbecco modified eagle medium (DMEM) and modified eagle medium (MEM) respectively supplemented with 10% fetal bovine serum (FBS) and 1% penicillin-streptomycin (Invitrogen Life Technologies, Carlsbad, California). The cell line was maintained in a humidified atmosphere of 5% CO_2 at 37 °C, with the medium changed every other day. A confluent monolayer was detached with trypsin and dissociated into a single cell suspension for further cell culture.

For fluorescence microscopy study, A431 or MCF7 cells (1×10^4) were cultured on the 35-mm MatTek glass-bottom culture dishes (Ashland, Massachusetts). After 24 h, the cells were washed with phosphate-buffered saline (PBS) and then incubated at 37 °C with Cy5.5-$Z_{EGFR:1907}$ (100 nM) for 1 h in dark. The EGFR-binding specificity of Cy5.5-$Z_{EGFR:1907}$ in cell culture was verified by incubating the A431 and MCF7 cells with or without large amounts of (blocking dose) nonfluorescent Ac-Cys-$Z_{EGFR:1907}$ peptide (10 μM). After the incubation period, cells were washed three times with ice-cold PBS. The fluorescence signal of the cells was recorded using an Axiovert 200M fluorescence microscope (Carl Zeiss Mi-

croImaging, Inc., Thornwood, New Jersey) equipped with a Cy5.5 filter set (Exciter, HQ 650/20 nm; Emitter, HQ 695/35 nm). An AttoArc HBO 100-W microscopic illuminator was used as a light source for fluorescence excitation. Images were taken using a thermoelectrically cooled charge-coupled device (CCD) (Micromax, model RTE/CCD-576, Princeton Instruments Inc., Trenton, New Jersey) and analyzed using MetaMorph Software version 6.2r4 (Molecular Devices Corporation, Downingtown, Pennsylvania).

2.4 *Binding Affinity Measurement with Flow Cytometry*

The flow cytometric analysis was performed as described in the literature with minor modification.[23] Samples were illuminated with a sapphire laser at 488 nm and a red laser at 635 nm on a BD FACSCalibur. The fluorescence and the forward-scattered and side-scattered light from 10,000 cells was detected at a rate of approximately 150 events/s. Flow cytometric data were analyzed with FACSDiva Software (BD Biosciences, San Jose, California). Prior to the flow cytometric analysis, A431 cells seeded in 75-cm^2 flasks approximately 3 days before the experiment were trypsinized [0.05% trypsin to 0.02% ethylenediaminetetraacetic acid (EDTA), 2.5 mL, ~10 min, 37 °C; Lonza Verviers S.P.R.L.] followed by a centrifugation (1000 g, 3 min). The pellet was subsequently resuspended in the binding buffer [PBS containing 1% bovine serum albumin (BSA) and 0.1% sodium azide (NaAz)]. A431 cells (0.2 M each, expressing $\sim 2 \times 10^6$ receptors/cell) were then distributed in Falcon tubes (15 mL). After centrifugation, the cells were incubated with 5 mL of Cy5.5-$Z_{EGFR:1907}$ at different concentrations (ranging from 0.1 to 100 nM) for 1 h at room temperature in the dark, with continuous rocking. The cells were then centrifuged (178 g, 4 min, 4 °C), washed with the binding buffer twice, resuspended in 500 μL of binding buffer, and subjected to flow cytometric analysis. All procedures after the incubation with the probe were performed on ice with ice-cold buffers. A triplicate of the flow cytometric data was analyzed with GraphPad Prism 5 (GraphPad Software, San Diego, California) and a nonlinear regression one-site-specific model was used to calculate the K_D of the probe.

2.5 *Optical Imaging of A431 Tumors in Mice*

All animal studies were carried out according to a protocol approved by the Stanford University Administrative Panels on Laboratory Animal Care (APLAC). Female athymic nude mice (nu/nu) at 4 to 6 weeks of age were injected subcutaneously in the shoulder with 5×10^6 A431 or MCF7 cells suspended in 100 μL of PBS. For the MCF7 mice model, 4.7 mg of estrogen was planted in the back 2 days before inoculation. The tumor-bearing mice were subjected to *in vivo* optical imaging studies 2 to 3 weeks after implantation.

In vivo fluorescence imaging was performed with an IVIS 200 small animal imaging system (Xenogen, Alameda, California). A Cy5.5 filter set (excitation 615 to 655 nm; emission 695 to 770 nm) was used for acquiring Cy5.5-$Z_{EGFR:1907}$ fluorescence *in vivo*. Identical illumination settings (lamp voltage, filters, *f*/stop, fields of view, binning) were used to acquire all images, and fluorescence emission was normalized to photons per second per centimeter squared per steradian (p/s/cm^2/sr). Images were acquired and analyzed using Living Image 3.0 software (Xenogen, Alameda, California). For the positive control experiment, mice ($n=3$) were injected via tail vein with 0.5 nmol of Cy5.5-$Z_{EGFR:1907}$ (20 nmol/kg) and subjected to optical imaging at various time points p.i. For the blocking experiment, mice ($n=3$ for each probe also) were injected with the mixture of 300 μg of Ac-Cys-$Z_{EGFR:1907}$ and 0.5 nmol of Cy5.5-$Z_{EGFR:1907}$. IVIS-200 NIR fluorescent images were acquired using a 1-s exposure time (*f*/stop=4, binning=4).

To subtract the autofluorescence, optical imaging using an IVIS spectrum small animal imaging system was also performed on mice for *ex vivo* imaging. The mice injected with Cy5.5-$Z_{EGFR:1907}$ were euthanized at 24 h p.i. and used for *ex vivo* fluorescence imaging. The tumor and other major tissues were dissected and placed on black papers. A slightly blue shifted excitation filters at 585 to 620 nm was used to measure the tissue autofluorescence. The background filter image was then subtracted from the primary filter image (excitation filter 620 to 655 nm) of Cy5.5-$Z_{EGFR:1907}$ fluorescence by image-math. IVIS-spectrum NIR fluorescent images were acquired using a 5-s exposure time (*f*/stop=4, binning=4) because of the much narrower emission filter range (710 to 730 nm). The fluorescence images were acquired, and mean fluorescence flux (p/s/cm^2/sr) for each sample was obtained.

2.6 *Statistical Analysis*

All the data are given as means ± SD (standard deviation) of n independent measurements. Statistical analysis was performed using a Student's t test. Statistical significance was assigned for P values <0.05. To determine tumor contrast, mean fluorescence intensities of the tumor area (T) at the shoulder of the animal and of the area (N) at the right flank (normal tissue) were calculated by the region-of-interest (ROI) function of Living Image software integrated with Igor (Wavemetrics, Lake Oswego, Oregon). Dividing T by N yielded the contrast between tumor tissue and normal tissue.

3 Results

3.1 *Synthesis of Cy5.5-$Z_{EGFR:1907}$*

The Affibody small protein Ac-Cys-$Z_{EGFR:1907}$ with a cysteine at the N terminal was successfully synthesized using a peptide synthesizer and purified by semipreparative HPLC. The peptide was generally obtained in 10% yield with over 95% purity [Fig. 1(a)]. The purified Ac-Cys-$Z_{EGFR:1907}$ was characterized by MALDI-TOF-MS. The measured molecular weight (MW) was consistent with the expected MW: $m/z=6690.0$ for $[M+H]^+$ (Calculated MW=6688.6). Ac-Cys-$Z_{EGFR:1907}$ was then conjugated with Cy5.5-mono-maleimide in the PBS buffer and purified by HPLC. MS analysis verified the success preparation of the final product Cy5.5-$Z_{EGFR:1907}$ (the observed MW: $m/z=7727.2$ for $[M+H]^+$, calculated $MW^+_{[M+Na]}=7727.4$). The purity for the final product was over 95% (retention time: 25 min) [Fig. 1(a)], and the recovery yield of the probe was 47%. Spectrum study showed that Cy5.5-$Z_{EGFR:1907}$ had similar absorption and fluorescence emission characteristics of free Cy5.5 dye, with $\lambda_{ab}=680$ nm and $\lambda_{em}=696$ nm [Fig. 1(b)].

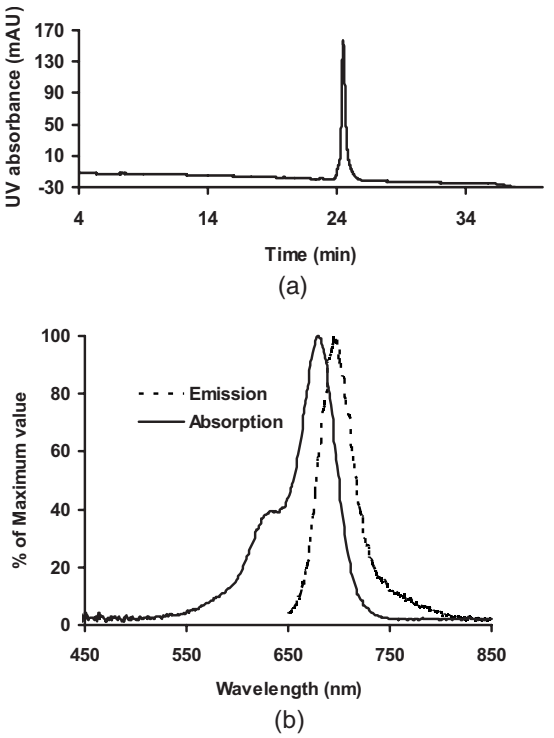

Fig. 1 (a) HPLC chromatogram of purified Cy5.5-$Z_{EGFR:1907}$ and (b) Absorption and emission fluorescence spectra of Cy5.5-$Z_{EGFR:1907}$.

3.2 *Binding Specificity and Affinity of Cy5.5-$Z_{EGFR:1907}$*

To demonstrate the EGFR specificity and subcellular localization of Cy5.5-$Z_{EGFR:1907}$, the probe was incubated with A431 tumor cells and fluorescent microscopic imaging was performed. With an 1 h incubation at 37 °C, intensive fluorescent signal was observed from the A431 cells membrane, and some of probe was also found to be inside of the cells (Fig. 2). Furthermore, the fluorescent signal from the cells could be significantly reduced by incubation of the cells with large excess of the Ac-Cys-$Z_{EGFR:1907}$ (10 μM), demonstrating the binding specificity of Cy5.5-$Z_{EGFR:1907}$ (Fig. 2). The staining of low EGFR expression MCF7 is barely visible. The flow cytometry study was performed for measurement of the binding affinity of Cy5.5-$Z_{EGFR:1907}$. A representative flow cytometric analysis was shown in Fig. 3(a). The equilibrium dissociation constant K_D was determined to be 43.6 ± 8.4 nM using a nonlinear regression one-site-specific model (Fig. 3(b)).

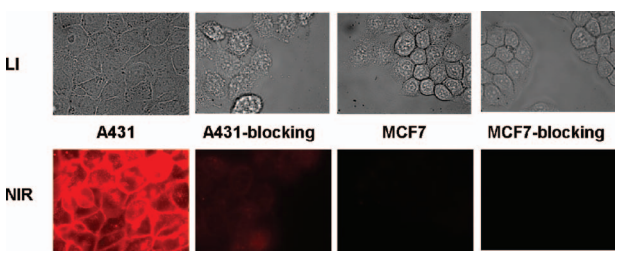

Fig. 2 Cell uptake of Cy5.5-$Z_{EGFR:1907}$ (100 nM) in A431 and MCF7 cells at 37 °C incubated with (blocking) or without the presence of the Affibody molecule Ac-Cys-$Z_{EGFR:1907}$ (10 μM). NIR fluorescent (NIR) and light images (LI) are shown at the top and bottom, respectively.

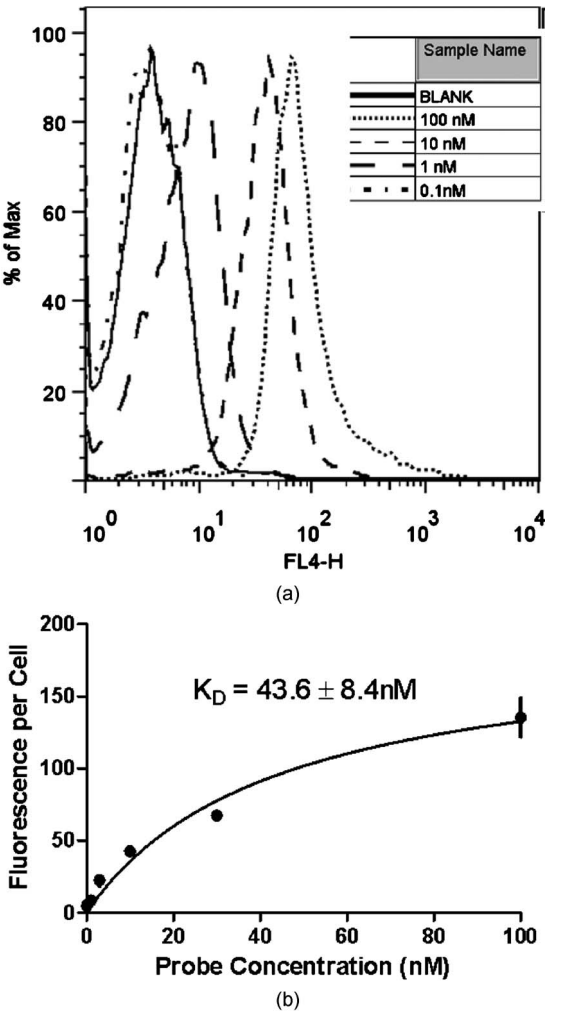

Fig. 3 (a) Flow cytometric analysis of Cy5.5-$Z_{EGFR:1907}$ binding to A431 cells at different concentrations (0.1 to 100 nM) and (b) cell population gated against a control blank, where triplicate data at each concentration were fitted with a nonlinear regression one-site- specific model.

3.3 *In Vivo and Ex Vivo Optical Imaging*

Figure 4(a) shows typical NIR fluorescent images of nude mice bearing subcutaneous A431 and MCF7 tumor after intravenous injection of 0.5 nmol of Cy5.5-$Z_{EGFR:1907}$. The A431 tumor could be clearly visualized from the surrounding background tissue from 0.5 to 4 h p.i.. Quantification analysis of ROIs was performed and the tumor to normal tissue ratio (T/N) as a function of time is depicted in Fig. 4(b). Cy5.5-$Z_{EGFR:1907}$ exhibited a fast tumor targeting property *in vivo*. The tumor-to-normal tissue ratio reached a peak at 2 h p.i. The receptor specificity of the probe was verified by the blocking experiment. Unlabeled Ac-Cys-$Z_{EGFR:1907}$ significantly reduced tumor uptake and tumor contrast at all the time points [Figure 4(a)]. Tumor contrast as quantified by ROI analysis of images indicated that the T/N value at 4 h p.i. was

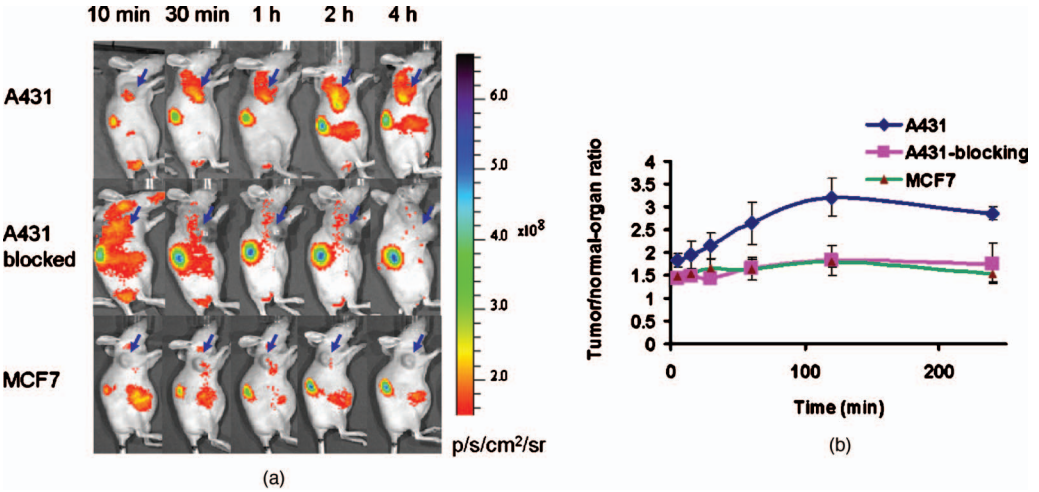

Fig. 4 (a) *In vivo* fluorescence IVIS-200 imaging of subcutaneous A431 and MCF7 tumor-bearing nude mice at 10 min, 30 min, 1 h, 2 h, and 4 h. Cy5.5-$Z_{EGFR:1907}$ (0.5 nmol) with (bottom) or without (top) coinjection of unlabeled Affibody $Z_{EGFR:1907}$ (300 μg) were injected. Arrows indicate the location of tumors. (b) ROI analysis of tumor-to-normal tissue ratios of Cy5.5-$Z_{EGFR:1907}$ in mice bearing A431 tumor at 10 min to 4 h p.i. (n=3).

reduced from 2.9 ± 0.1 to 1.8 ± 0.4 ($P < 0.05$). At 4 h p.i., MCF7 tumor showed much lower T/N value (1.54 ± 0.19).

The result for *ex vivo* tumor mice imaging at 24 h p.i., as shown in Fig. 5(a). Quantitative analysis showed that there is also large amount of probe trapped inside the kidney without clearance [Fig. 5(b)]. The tumor-to-normal organ (except kidney) ratios are also high [Fig. 5(c)]. For example, the ratios for tumor-to-lung and tumor-to-muscle are 5.6 ± 1.8 and 6.5 ± 0.4, respectively.

4 Discussion

NIR fluorescent imaging, which uses neither ionizing radiation nor radioactive materials, is emerging as a promising modality that can complement traditional nuclear imaging methods. Optical molecular probes with high sensitivity, stability, fast targeting, and rapid clearance could be prepared.[17,24,25] Furthermore, optical imaging has very high resolution and shows great potential in clinical translation because of (1) the easy visualization of targeted tissues and (2) its use as supplementary visual aide to provide guidance in surgery.[26] Anti-EGFR Affibody, $Z_{EGFR:1907}$, was radiolabeled with ^{64}Cu in our recent study, which demonstrated good and fast tumor uptake and long retention.[21] It is also of a great interest to us to apply this Affibody molecule for developing an optical imaging probe, since there is a high demand for an EGFR-targeted optical probe with an ideal *in vivo* imaging profile.

To achieve this goal, Affibody analog Cys-$Z_{EGFR:1907}$ was synthesized to render site-specific labeling using maleimide chemistry. Conjugation of the small protein with Cy5.5-mono-maleimide was successfully achieved, moreover the absorption and emission fluorescence properties of the probe remain very close to the unconjugated dye (Fig. 1). The probe

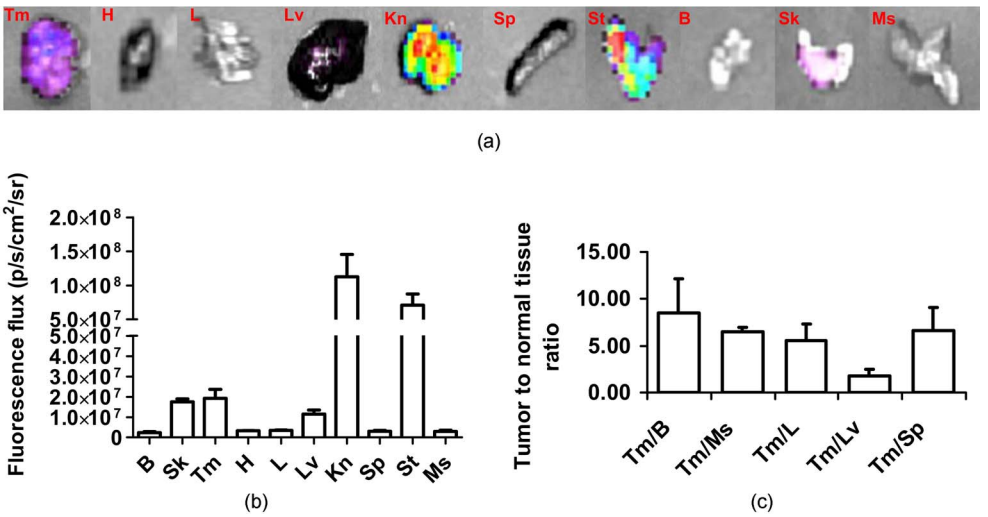

Fig. 5 (a) *Ex vivo* imaging of tumor and normal tissues of Cy5.5-$Z_{EGFR:1907}$ after sacrificed the mice at 24 h p.i.: Tm, tumor; H, heart; L, lung; Lv, liver; Kn, kidney; Sp, spleen; St, stomach; B, blood; Sk, skin; Ms, Muscle. (B) ROI analysis of fluorescent signal from tumor and normal tissues. (b) Fluorescence intensity ratios of tumor-to-normal tissues based on the ROI analysis. Error bar was calculated as the standard deviation (n=3).

Cy5.5-$Z_{EGFR:1907}$ also showed good binding affinity to the A431 cell surface EGFR with a K_D value of 43.6 ± 8.4 nM, which is considered sufficient for further *in vivo* evaluation, although target avidity was lower than that of the unmodified Affibody $Z_{EGFR:1907}$ (~ 5 nM)[20] [Fig. 3(b)]. This result implies that the Affibody protein tolerates some *N* terminal modifications. Fluorescent microscopy of Cy5.5-$Z_{EGFR:1907}$ showed that the majority of the probe bond to cell surface receptors after 1 h incubation, indicating the slow internalization of the Affibody molecule, which is also consistent with previous finding of the radioactive counterpart.[20,21] More importantly, the specificity of the probe was verified with blocking by unlabeled Affibody (Fig. 2). These results warranted the further evaluation of the probe for *in vivo* EGFR-targeted tumor imaging.

Considering the high sensitivity of *in vivo* NIR imaging, 0.5 nmol of Cy5.5-$Z_{EGFR:1907}$ was injected into A431 mice, and optical imaging studies were performed using IVIS-200 systems. Consistent with our expectation, good tumor uptakes and imaging qualities were observed [Fig. 4(a)]. The A431 tumor was clearly delineated from normal tissues at as early as 0.5 h p.i. Quantification analysis of IVIS-200 images illustrated that tumor uptake reach plateau at 2 h [Fig. 4(b)]. These results were attributable to the fast tumor targeting and rapid blood clearance abilities of Affibody molecules. Kidney uptake was also very high even at 24 h p.i., which is consisted with the radiometal labeled Affibody probes.[20,21,27] Further *ex vivo* imaging study exhibited that tumor-to-blood ratio reached 8.5 ± 3.6 at 24 h p.i. Autofluorescence was very obvious for the skin, which increases the background. *Ex vivo* imaging also revealed that tumor-to-muscle ratio was as high as 6.5 ± 0.4. These properties are favorable and demonstrate the use of the optical probe for intraoperative optical imaging.

In vivo optical imaging of EGFR has extensively been investigated using monoclonal antibody such as cetuximab (Erbitux) labeled with NIR dyes.[8,9,28] Cy5.5-labeled cetuximab (abbreviated as Cy5.5-Erbitux) was reported to target EGFR-high-expression MDA-MB-231 tumors and reached a maximum tumor to normal tissue ratio of ca 3 at 24 h p.i.. However, because of the slow localization and clearance of the antibody, Cy5.5-Erbitux showed almost no difference between MDA-MB-231 tumor with high EGFR expression and MCF-7 with low expression[9] before 6 h p.i. In contrast, Cy5.5-$Z_{EGFR:1907}$ demonstrated fast tumor accumulation (T/N ratio$=2.64 \pm 0.46$ at 1 h p.i.) in the A431 model, while accumulation was very low in MCF7 tumor (T/N ratio $=1.62 \pm 0.22$ at 1 h p.i., $P < 0.05$), which is advantageous for both preclinical and clinical applications. NIR-dye-labeled EGF protein has also been reported for *in vivo* imaging.[29,30] However, EGF as a natural ligand has some side effects such as stimulation of EGFR phosphorylation, causing vomiting and diarrhea.[30,31] Finally, quantum dot conjugated with reduced EGF (r-Egf) was also reported, but the imaging result was poor and toxicity of quantum dot was a concern even at very low amount.[32]

5 Conclusion

Cy5.5-$Z_{EGFR:1907}$ provided high-sensitivity, receptor-specific molecular imaging of EGFR-positive tumors. It showed good tumor-to-normal tissue ratios, fast tumor targeting ability, and quick blood clearance. Cy5.5-$Z_{EGFR:1907}$ is a promising probe for further applications in EGFR-targeted optical imaging.

Acknowledgments

This work was supported, in part, by the California Breast Cancer Research Program 14IB-0091 (Z.C.) and an SNM Pilot Research Grant (to Z.C.). We also would like to thank Steven Jing for the help with Affibody synthesis and purification and Edwin Chang for helpful discussions.

References

1. F. X. Real, W. J. Rettig, P. G. Chesa, M. R. Melamed, L. J. Old, and J. Mendelsohn, "Expression of epidermal growth factor receptor in human cultured cells and tissues," *Cancer Res.* **46**(9), 4726–4731 (1986).
2. E. Van Cutsem, C. H. Köhne, E. Hitre, J. Zaluski, C. R. Chang Chien, A. Makhson, G. D'Haens, T. Pintér, R. Lim, G. Bodoky, J. K. Roh, G. Folprecht, P. Ruff, C. Stroh, S. Tejpar, M. Schlichting, J. Nippgen, and P. Rougier, "Cetuximab and chemotherapy as initial treatment for metastatic colorectal cancer," *N. Engl. J. Med.* **360**(14), 1408–1417 (2009).
3. J. G. Paez, P. A. Jänne, J. C. Lee, S. Tracy, H. Greulich, S. Gabriel, P. Herman, F. J. Kaye, N. Lindeman, T. J. Boggon, K. Naoki, H. Sasaki, Y. Fujii, M. J. Eck, W. R. Sellers, B. E. Johnson, and M. Meyerson, "EGFR mutations in lung cancer: correlation with clinical response to gefitinib therapy," *Science* **304**(5676), 1497–1500 (2004).
4. M. H. Cohen, J. R. Johnson, Y. F. Chen, R. Sridhara, and R. Pazdur, "FDA drug approval summary: erlotinib (Tarceva) tablets," *Oncologist* **10**, 461–466 (2005).
5. H. Su, Y. Seimbille, G. Z. Ferl, C. Bodenstein, B. Fueger, K. J. Kim, Y. T. Hsu, S. M. Dubinett, M. E. Phelps, J. Czernin, and W. A. Weber, "Evaluation of [^{18}F]gefitinib as a molecular imaging probe for the assessment of the epidermal growth factor receptor status in malignant tumors," *Eur. J. Nucl. Med. Mol. Imaging* **35**(6), 1089–1099 (2008).
6. A. Pal, A. Glekas, M. Doubrovin, J. Balatoni, T. Beresten, D. Maxwell, S. Soghomonyan, A. Shavrin, L. Ageyeva, R. Finn, S. M. Larson, W. Bornmann, and J. G. Gelovani, "Molecular imaging of EGFR kinase activity in tumors with ^{124}I-labeled small molecular tracer and positron emission tomography," *Mol. Imaging Biol.* **8**(5), 262–277 (2006).
7. H. Wang, J. Yu, G. Yang, X. Song, X. Sun, S. Zhao, and D. Mu, "Assessment of ^{11}C-labeled-4-N-(3-bromoanilino)-6,7-dimethoxyquinazoline as a positron emission tomography agent to monitor epidermal growth factor receptor expression," *Cancer Sci.* **98**(9), 1413–1416 (2007).
8. J. P. Gleysteen, J. R. Newman, D. Chhieng, A. Frost, K. R. Zinn, and E. L. Rosenthal, "Fluorescent labeled anti-EGFR antibody for identification of regional and distant metastasis in a preclinical xenograft model," *Head Neck* **30**(6), 782–789 (2008).
9. K. Wang, K. Wang, W. Li, T. Huang, R. Li, D. Wang, B. Shen, and X. Chen, "Characterizing breast cancer xenograft epidermal growth factor receptor expression by using near-infrared optical imaging," *Acta Radiol.* **11**, 1–9 (2009).
10. C. R. Divgi, S. Welt, M. Kris, F. X. Real, S. D. J. Yeh, R. Gralla, B. Merchant, S. Schweighart, M. Unger, S. M. Larson, and J. Mendelsohn, "Phase I and imaging trial of indium-111-labeled anti-epidermal growth factor receptor monoclonal antibody 225 in patients with squamous cell lung carcinoma," *J. Natl. Cancer. Inst. (Bethesda)* **83**(2), 97–104 (1991).
11. R. J. Hosse, A. Rothe, and B. E. Power, "A new generation of protein display scaffolds for molecular recognition," *Protein Sci.* **15**, 14–27 (2006).
12. H. K. Binz, P. Amstutz, and A. Pluckthun, "Engineering novel binding proteins from nonimmunoglobulin domains," *Nat. Biotechnol.* **23**(10), 1257–1268 (2005).
13. K. Nord, E. Gunneriusson, J. Ringdahl, S. Ståhl, M. Uhlén, and P. Å. Nygren, "Binding proteins selected from combinatorial libraries of an alpha-helical bacterial receptor domain," *Nat. Biotechnol.* **15**(8), 772–777 (1997).
14. A. Orlova, V. Tolmachev, R. Pehrson, M. Lindborg, T. Tran, M. Sandström, F. Y. Nilsson, A. Wennborg, L. Abrahmsén, and J. Feld-

wisch, "Synthetic affibody molecules: a novel class of affinity ligands for molecular imaging of HER2-expressing malignant tumors," *Cancer Res.* **67**(5), 2178–2186 (2007).
15. V. Tolmachev, A. Orlova, R. Pehrson, J. Galli, B. Baastrup, K. Andersson, M. Sandström, D. Rosik, J. Carlsson, H. Lundqvist, A. Wennborg, and F. Y. Nilsson, "Radionuclide therapy of HER2-positive microxenografts using a 177Lu-labeled HER2-specific Affibody molecule," *Cancer Res.* **67**(6), 2773–2782 (2007).
16. Z. Cheng, O. P. De Jesus, M. Namavari, A. De, J. Levi, J. M. Webster, R. Zhang, B. Lee, F. A. Syud, and S. S. Gambhir, "Small-animal PET imaging of human epidermal growth factor receptor type 2 expression with site-specific 18F-labeled protein scaffold molecules," *J. Nucl. Med.* **49**(5), 804–813 (2008).
17. S. B. Lee, M. Hassan, R. Fisher, O. Chertov, V. Chernomordik, G. Kramer-Marek, A. Gandjbakhche, and J. Capala, "Affibody molecules for in vivo characterization of HER2-positive tumors by near-infrared imaging," *Clin. Cancer Res.* **14**(12), 3840–3849 (2008).
18. R. P. Baum, A. Orlova, V. Tolmachev, and J. Feldwisch, "Receptor PET/CT and SPECT using an Affibody molecule for targeting and molecular imaging of HER2-positive cancer in animal xenografts and human breast cancer patients [abstract]," *J. Nucl. Med.* **47**(Supp. l), 108P (2006).
19. T. Engfeldt, B. Renberg, H. Brumer, P. Å. Nygren, and A. E. Karlström, "Chemical synthesis of triple-labelled three-helix bundle binding proteins for specific fluorescent detection of unlabelled protein," *ChemBioChem* **6**(6), 1043–1050 (2005).
20. M. Friedman, A. Orlova, E. Johansson, T. L. Eriksson, I. Höidén-Guthenberg, V. Tolmachev, F. Y. Nilsson, and S. Ståhl, "Directed evolution to low nanomolar affinity of a tumor-targeting epidermal growth factor receptor-binding Affibody molecule," *J. Mol. Biol.* **376**(5), 1388–1402 (2008).
21. Z. Miao, G. Ren, H. Liu, L. Jiang, and Z. Cheng, "Small-animal PET imaging of human epidermal growth factor receptor positive tumor with a ^{64}Cu labeled affibody protein," *Bioconjugate Chem.* **21**(5), 947–954 (2010).
22. Z. Miao, G. Ren, H. Liu, L. Jiang, S. S. Gambhir, and Z. Cheng, "A protein scaffold based molecule for EGFR PET imaging," *J. Nucl. Med.* **50**(supplement 2), 386 (2009) (Abstract).
23. V. Tolmachev, M. Friedman, M. Sandström, T. L. Eriksson, D. Rosik, M. Hodik, S. Ståhl, F. Y. Frejd, and A. Orlova, "Affibody molecules for epidermal growth factor receptor targeting in vivo: aspects of dimerization and labeling chemistry," *J. Nucl. Med.* **50**(2), 274–283 (2009).
24. T. Troy, D. Jekic-McMullen, L. Sambucetti, and B. Rice, "Quantitative comparison of the sensitivity of detection of fluorescent and bioluminescent reporters in animal models," *Mol. Imaging* **3**(1), 9–23 (2004).
25. Z. Cheng, Y. Wu, Z. Xiong, S. S. Gambhir, and X. Chen, "Near-infrared fluorescent RGD peptides for optical imaging of integrin $\alpha_v\beta_3$ expression in living mice," *Bioconjugate Chem.* **16**(6), 1433–1441 (2005).
26. A. Nakayama, F. del Monte, R. J. Hajjar, and J. V. Frangioni, "Functional near-infrared fluorescence imaging for cardiac surgery and targeted gene therapy," *Mol. Imaging* **1**(4), 365–77 (2002).
27. Z. Cheng, O. P. De Jesus, D. J. Kramer, A. De, J. M. Webster, O. Gheysens, J. Levi, M. Namavari, S. Wang, J. M. Park, R. Zhang, H. Liu, B. Lee, F. A. Syud, and S. S. Gambhir, "^{64}Cu-labeled Affibody molecules for imaging of HER2 expressing tumors," *Mol. Imaging Biol.* **12**, 316–324 (2009).
28. K. P. Withrow, J. R. Newman, J. B. Skipper, J. P. Gleysteen, J. S. Magnuson, K. Zinn, and E. L. Rosenthal, "Assessment of bevacizumab conjugated to Cy5.5 for detection of head and neck cancer xenografts," *Technol. Cancer Res. Treat.* **7**(1), 61–66 (2008).
29. S. Ke, X. Wen, M. Gurfinkel, C. Charnsangavej, S. Wallace, E. M. Sevick-Muraca, and C. Li, "Near-infrared optical imaging of epidermal growth factor receptor in breast cancer xenografts," *Cancer Res.* **63**(22), 7870–7875 (2003).
30. K. E. Adams, S. Ke, S. Kwon, F. Liang, Z. Fan, Y. Lu, K. Hirschi, M. E. Mawad, M. A. Barry, and E. M. Sevick-Muraca, "Comparison of visible and near-infrared wavelength-excitable fluorescent dyes for molecular imaging of cancer," *J. Biomed. Opt.* **12**(2), 024017 (2007).
31. A. Cuartero-Plaza, E. Martínez-Miralles, R. Rosell, C. Vadell-Nadal, M. Farré, and F. X. Real, "Radiolocalization of squamous lung carcinoma with ^{131}I-labeled epidermal growth factor," *Clin. Cancer Res.* **2**(1), 13–20 (1996).
32. P. Diagaradjane, J. M. Orenstein-Cardona, N. E. Colón-Casasnovas, A. Deorukhkar, S. Shentu, N. Kuno, D. L. Schwartz, J. G. Gelovani, and S. Krishnan, "Imaging epidermal growth factor receptor expression *in vivo*: pharmacokinetic and biodistribution characterization of a bioconjugated quantum dot nanoprobe," *Clin. Cancer Res.* **14**(3), 731–741 (2008).